AN OPTIMIZED DC-TO-DC CONVERTER TOPOLOGY FOR HIGH-VOLTAGE PULSE-LOAD APPLICATIONS

V. García * , M. Rico * , J. Sebastián *, M. Mª. Hernando * and J. Uceda **

* Universidad de Oviedo. Dpto. de Ingeniería Electrónica.
ETSII. Campus de Viesques - 33204 - GIJON. ASTURIAS. SPAIN.
phone: (348)-5182087 fax: (348)-5338538

** Universidad Politécnica de Madrid. Div. Ingeniería Electrónica
ETSII. c/ José Gutierrez Abascal nº 2 - 28006 - MADRID. SPAIN.
phone: (341)-5645972 fax: (341)-5645966

Abstract: This paper presents the study of a high-voltage dc-to-dc resonant converter which has excellent behaviours to be used in applications with strong variations in the output voltage and in the output current, because it maintains high efficiency in these types of applications. To do so, the switching losses have been minimized by integrating all parasitic elements (leakage inductance, secondary side capacitance of the high-voltage transformer and parasitic capacitances of the power switches and diodes) into the power topology, and the conduction losses have been minimized by operating the converter in a special mode (Optimum Switching Line) in which no reactive energy is returned from the resonant elements to the input voltage source. The type of control used (PWM Phase-Shifted) allows one to maintains these desirable characteristics even when the operating point suffers a very strong variation. The final power topology might be called a "Full-Bridge, Champed Mode, LCC-Type Parallel Resonant Converter with Capacitive Output Filter".

INTRODUCTION

High-voltage dc-to-dc converters are usually used in very different types of electronic equipment. Typical examples are telecommunication equipment with vacuum tubes (like Travelling Wave Tube (TWT) amplifiers), CO_2 laser-based systems for industrial applications and X-ray equipment.

Many power converters have been proposed in the last twenty years as a means of supplying high output voltages. The common goals of all of them have been reliability, high efficiency and low cost and size. Converters with line transformers (like Cockroft-Walton rectifiers) were useless in spacecraft communication systems so several high-voltage dc-to-dc switching power converters were developed for communication satellites [1], [2] and [3], and they were used afterwards in other applications. Initially, all of these converters were PWM type (not-resonant converters). However, the high-voltage transformers used in them caused several serious problems in the PWM power topologies. The large turns ratio of the transformer exacerbates the transformer nonidealities (see figure 1). In particular, the leakage inductance L_l and the parasitic capacitance C_p (formed of the secondary winding capacitance C_{sw} and the diode capacitances C_D) can significantly change converter behaviour. The former causes undesirable voltage spikes which can damage circuit components, and the latter results in current spikes and slow risetimes.

An attractive alternative for high-voltage dc-to-dc applications is the use of a resonant converter in which the transformer nonidealities are incorporated into the basic operation of the circuit. One might then attempt to use the leakage inductance and winding capacitance partially or wholly as resonant tank elements, and thereby turn these nonidealities into useful articles. Such a converter should function efficiently and reliably [4].

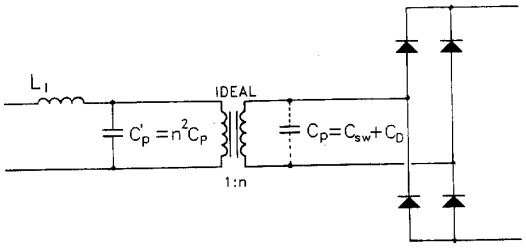

Figure 1. High-voltage transformer and rectifier

One of the resonant dc-to-dc converter used for high-voltage applications is the Series Resonant Converter (SRC) shown in figure 2a. As this figure shows, the transformer leakage inductance L_l is integrated into the power topology because it contributes to the resonant inductance L_R.

The resonant capacitor C_R avoids possible saturation problems in the transformer. However, the parasitic capacitance C'_p is not placed in parallel with the resonant capacitor C_R and it is not integrated into the power topology. Although this fact limits the use of this topology in high-voltage applications, the SRC has nevertheless been used in high-voltage, high-power converters for X-ray generators [5], [6].

The Parallel Resonant Converter (PRC) overcomes SRC problems because it integrates the parasitic capacitance C'_p as resonant capacitor C_R in the power topology. PRC converters used in low output voltage applications have a LC-type output filter. However the output filter inductor can become a large and expensive component in high-voltage applications, comparable in size to the high voltage transformer. Fotunately, it is possible to remove this component altogether, without degrading the performance of the converter, [4], obtaining the converter shown in figure 2b. Some practical designs can be seen in references [7] and [8]. However, the PRC with capacitive output filter presents several limitations. For example saturation problems in the high-voltage transformer can occur in the full-bridge implementation of the PRC (but not in the

0-7803-1859-5/94/$4.00 © 1994 IEEE

half-bridge). To avoid this problem, the easiest solution is to place a blocking capacitor C_B in series with the transformer (see figure 2.c). If the value of this capacitor has the same order of magnitude as the capacitor C'_P, then the new converter becomes another converter - the hybrid Series-Parallel Resonant Converter (SPRC) also called LCC-Type Parallel Resonant Converter [9] - in which there are two resonant capacitances: $C_{R1}=C_B$ and $C_{R2}=C'_P$.

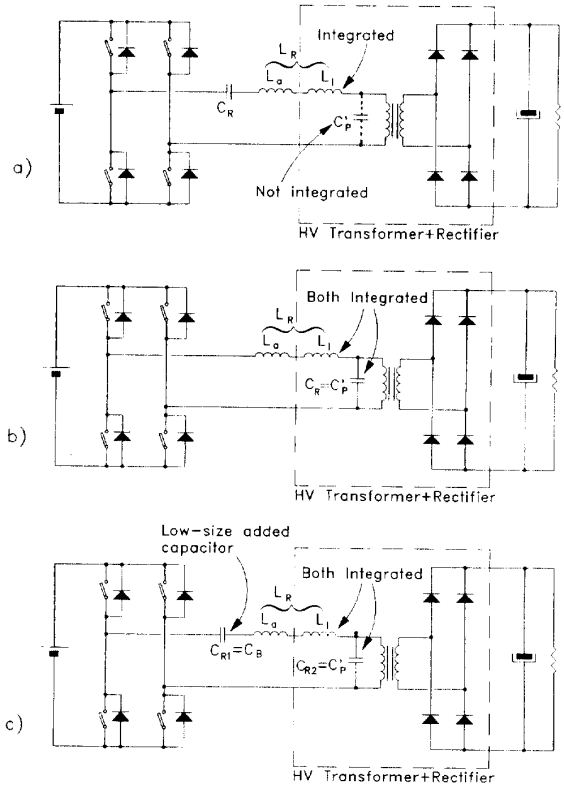

Figure 2. Some dc to dc converters used in high-voltage applications a) Series Resonant Converter b) Parallel Resonant Converter c) Hybrid Series- Parallel Resonant Converter

The second PRC limitation is that the current carried by the power switches and resonant components is relatively independent of the load, [10] and [11]. The consequence of this behaviour is that the conduction losses in the switches and in the reactive components stay relatively fixed as the load decreases so the light-load efficiency of the converter suffers. Thus this converter is less than ideal for applications which have large input or output voltage ranges and which require it to operate considerably below its maximum design power while maintaining very high efficiency.

The above problem can be reduced using a SPRC. But some high-voltage applications require a considerable variation in the converter operation point. Laser systems employed for cutting, marking or surface treatment, or X-ray equipment are typical examples. To achieve efficient operation in these cases, the usual switching frequency control is not useful. In contrast, the PWM Phase-Shifted control (also called Clamped Mode) has been successfully used to control PRCs both with LC output filter [12] and even with capacitive output filter [8]. However, this type of control as applied to the SPRC with capacitive output filter has yet to be studied.

In summary, the hybrid Series-Parallel Resonant Converter (SPRC) with capacitive output filter and with PWM Phase-Shifted control seems to be the optimum power converter for high-voltage, pulse-load applications because:

- It integrates all the main transformer and rectifier parasitics.
- It has a small-size blocking capacitor connected in series with the high-voltage transformer.
- Even the capacitances of the power switches can be integrated in lossless snubbers [11], [12], [13], as we will show in the following section, if forced turn-off (turn-off with positive current) is achieved in the four power switches.
- Operation with no reactive energy returned to the input voltage source can be achieved with Phase-Shifted PWM control, even with considerable variations in the output voltage and load. High efficiency can thus be obtained in such conditions.

STEADY-STATE ANALYSIS OF THE PROPOSED CONVERTER

The converter proposed above and the nomenclature used in the analysis can be seen in figure 3, where L_{R1}, C_{R1} and C_{R2} constitute the resonant circuit, T is an ideal transformer and C_F is the output filter. The voltage in this capacitor will be taken as constant in each switching period, and, therefore, the capacitor will be substituted by a dc voltage source U_0 in the analysis. All of the elements shown in figure 3 will be considered ideal.

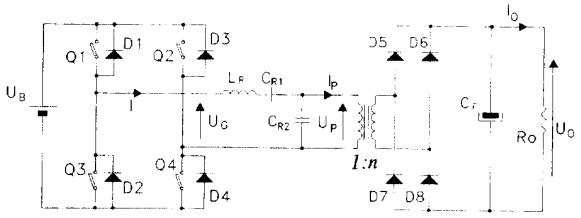

Figure 3. Proposed converter

The different conduction states in the four controlled switches (Q_1-Q_4), in their anti-parallel diodes (D_1-D_4), and in the output rectifier diodes (D_5-D_8), give rise to the nine equivalent circuits shown in figure 4.

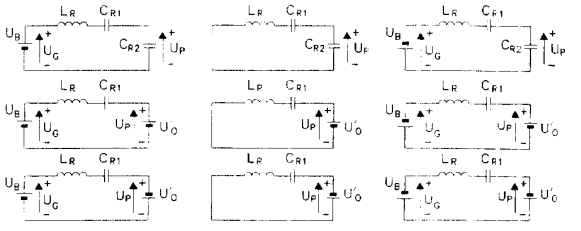

Figure 4. Equivalent circuits used in the analysis of the converter shown in figure 3. $U'_0=U_0/n$ in this figure.

It should be noted that there are three equivalent circuits in which the voltage U_G applied to the resonant circuit is zero (there is no input voltage source U_B). They characterize the

typical phase-shifted PWM control, as can be seen in figure 5, where U_G is zero during a π-θ angle.

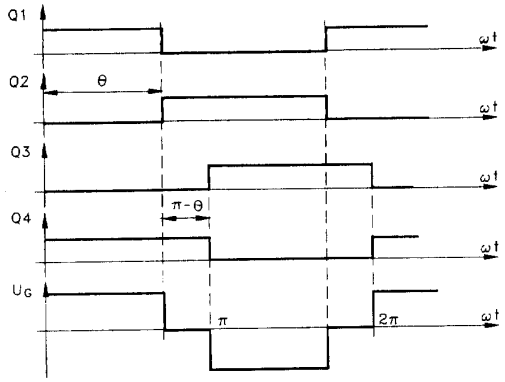

Figure 5. Typical waveforms in phase-shifted PWM control

The nine equivalent circuits give rise to several operation modes (defined as the sequential connection of several of the nine equivalent circuits). Therefore, the analysis complexity is very high and a method to resolve the circuit operation without losing the physical behaviour of the converter must be found.

All the possible evolutions in the converter can be classified according to commutation types. The converter has four commutations in each period, two in each inverter branch; however since both the circuit and the drive waveform are simmetrical, the circuit analysis during a half period (two commutations per half cycle or one commutation per inverter branch) can be carried out. The direction of the resonant current during the commutation time defines the commutation types, so that the operation modes can be divided into three types:

* **Operation modes with N-Type Commutation** (Natural turn-off in the four switches).

Each power switch must turn on when the antiparallel diode of the other switch in the same branch is carrying the resonant current. Each power switch turns off when the resonant current reaches zero value. In this case the most adequate switch is a thyristor type. Typical waveforms in N-Type Commutation are shown in figure 6.

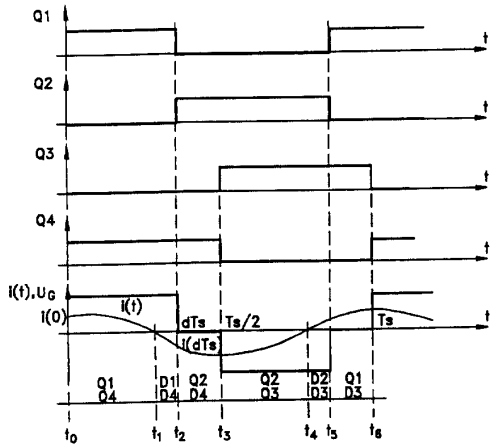

Figure 6. Waveforms in N-Type Commutation

* **Operation modes with F-Type Commutation** (Forced turn-off in the four switches).

Each power switch must turn-on when the resonant current reaches zero value in its antiparallel diode and it must turn off forced by its driving signal while it is carrying the resonant current. In this case the most adequate switch is a transistor type (BJTs, MOSFETs and IGBTs). An additional advantage can also be achieved: it is possible to incorporate slower antiparallel diodes and non-disipative snubbers (simple lossless capacitor snubbers) in all the switches. Typical waveforms in F-Type Commutation are shown in figure 7.

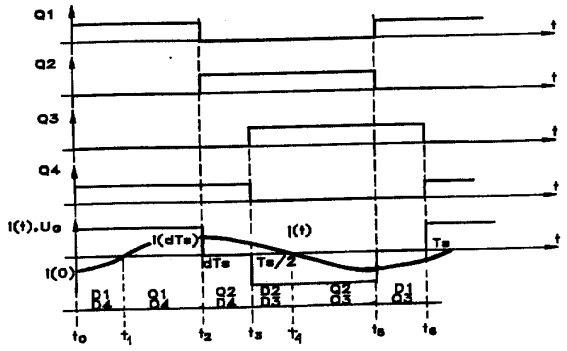

Figure 7. Waveforms in F-Type Commutation

* **Operation modes with M-Type Commutation** (Mixed Natural and Forced turn-off).

One branch commutes as an N-Type while the other one commutes as an F-Type. Typical waveforms in M-Type Commutation are shown in figure 8. Note that the energy flowing into the circuit in M-Type Commutation must always be incoming. That is to say, no energy exchange with the primary input source exists in M-Type Commutation.

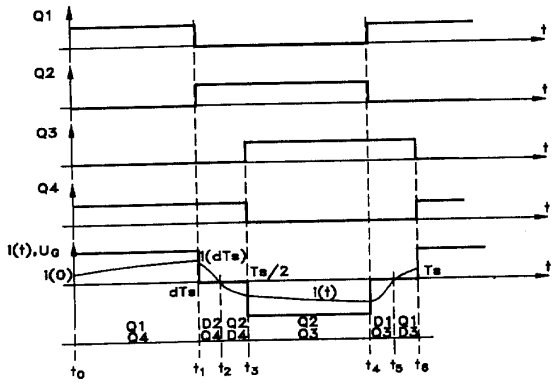

Figure 8. Waveforms in M-type Commutation

To carry out the converter analysis, the electrical magnitudes have been normalized using the following base values:

- Base voltage: The input voltage source: U_B

- Base frequency: $f=\frac{1}{2\pi\sqrt{L_B C_B}}=\frac{\omega}{2\pi}$

- Base impedance: $Z=\sqrt{L_B/C_B}$

- Base current: $I=U_B/Z$

where C_R is the series connection of both resonant capacitors:

$$C_R=\frac{C_{R1}C_{R2}}{C_{R1}+C_{R2}}$$

All the circuits shown in figure 4 can be reduced to only two general circuits, named **Circuit A** and **Circuit B** as it is shown in figure 9. Mathematical equations obtained from these two general circuits in normalized values (lower-case letters) are:

Equations from circuit A:

$$i(t)=i(t_i)\cos\omega(t-t_i)+[u_G-u_C(t_i)]\sin\omega(t-t_i) \quad [1]$$

$$u_C(t)=u_G+i(t_i)\sin\omega(t-t_i)-[u_G-u_C(t_i)]\cos\omega(t-t_i) \quad [2]$$

$$u_{C2}(t)=u_{C2}(t_i)+a[(u_G-u_C(t_i))(1-\cos\omega(t-t_i)+i(t_i)\sin\omega(t-t_i)] \quad [3]$$

where:

$$a=\frac{C_R}{C_{R2}} \quad [4]$$

$$u_G=\pm 1 \quad [5]$$

Equations from circuit B:

$$i(t)=i(t_i)\cos\omega'(t-t_i)+\frac{u_G-u_t-u_{C1}(t_i)}{B}\sin\omega'(t-t_i) \quad [6]$$

$$u_C(t)=u_G+Bi(t_i)\sin\omega'(t-t_i)-[u_G-u_t-u_{C1}(t_i)]\cos\omega'(t-t_i) \quad [7]$$

$$u_{C2}(t)=u_t=\pm u'_0 \quad [8]$$

where:

$$\omega'=\omega\sqrt{\frac{C_R}{C_{R1}}} \quad [9]$$

$$B=\frac{\omega'}{\omega} \quad [10]$$

and t_i is the initial time.

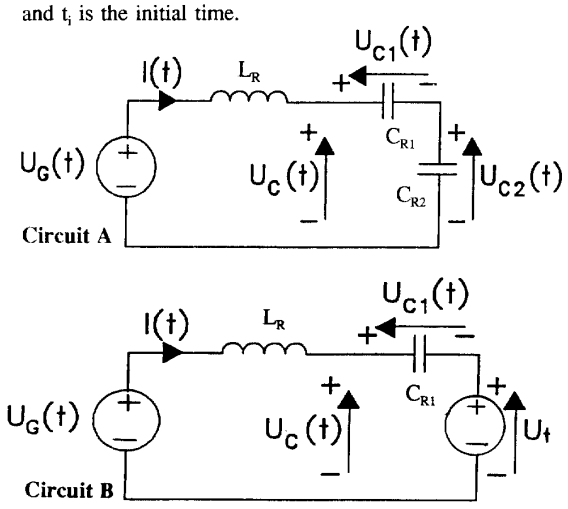

Figure 9. General circuits A and B

Firstly, the no-load and shortcircuit conditions in the converter were analized in order to delimit the converter operation area. The maximum output voltage and the maximum output current were thus found. Both output voltage and current are established from these two limits in any load condition.

Equations to solve the no-load condition can be obtained from **Circuit A** (**Circuit B** is not possible in this operation mode). The two possible waveforms in no-load operation are shown in figure 10. One of these waveforms corresponds to N-Type Commutation and has been marked NIII mode; the other one corresponds to F-type Commutation and has been marked FIII mode. It is important to note that in no-load condition M-type Commutation is not possible (from the energy-balance point of view).

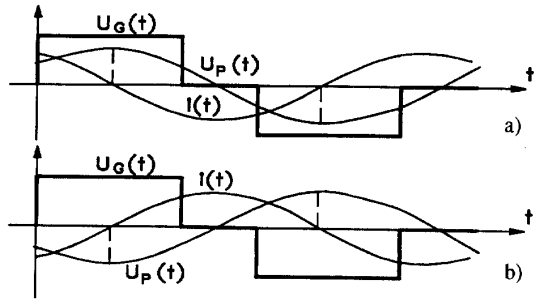

Figure 10. Waveforms in no-load operation: a) NIII (below resonance) b) FIII (above resonance)

On the other hand, equations to solve the shortcircuit condition can be obtained from **Circuit B** with U_t value equal to zero (in this case **Circuit A** is not possible). The resonant frequency for this circuit involves only the C_{R1} capacitor (the C_{R2} capacitor is shortcircuited) and it has been marked by the letter "B" in per unit value.

The two possible waveforms in shortcircuit operation are shown in figure 11. As in no-load condition, one of these waveforms corresponds to N-Type Commutation and has been marked NI mode; the other one correspond to F-type Commutation and has been marked FI mode. It is important to note that in shortcircuit condition the M-type Commutation is not possible (as from the energy-balance point of view).

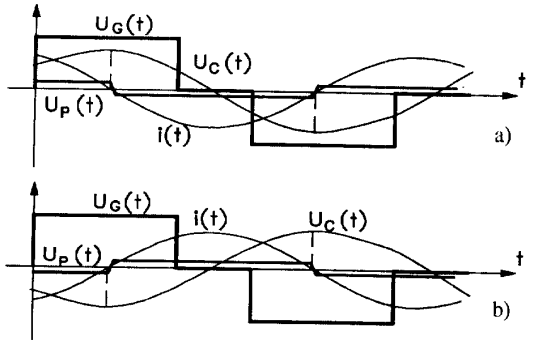

Figure 11. Waveforms in shortcircuit operation: a) NI (below resonance) b) FI (above resonance)

Figure 12 shows a typical operation area in per unit values (it is possible to obtain a different operation area with different duty cycle values (d) and with different parameter "a" values). The upper side of the figure shows the output voltage in no-

load conditions. It is important to emphasize that the NIII mode exists below the resonant frequency ($f_{sn}=f_s/f_n=1$) and the FIII mode exists above it.

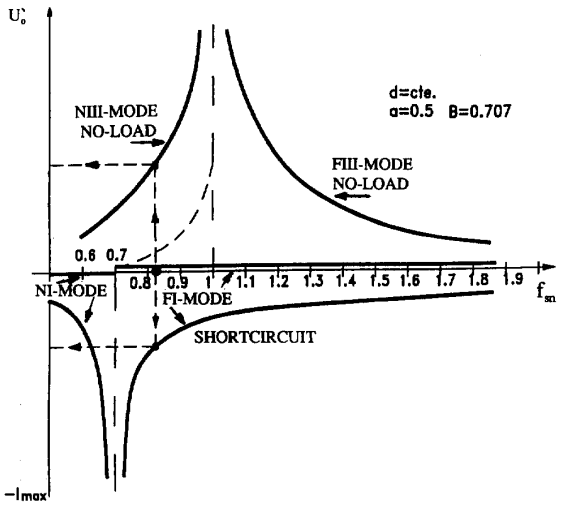

Figure 12. Upper side: output voltage in no-load condition
Lower side: output current in shortcircuit condition

The lower side shows the output current in shortcircuit conditions. In the same way, it is important to emphasize that the NI mode exists below the shortcircuit resonance frequency and the FI mode exists above it.

When the operating point of the converter moves from N-Types to F-Types in no-load and shortcircuit conditions both respective resonance frecuencies must be crossed. In load condition the only way from N-Types to F-Types is by crossing through M-Types; moreover this zone must correspond with the resonance region (the energy flows into the circuit). This is very important because it delimits the zone where N-Type, F-type and M-type Commutations exist.

A more detailed analysis allows one to determine the existence of 3 different modes to each commutation type depending on the time in which the resonant voltage in the capacitor C_{R2} reaches the output voltage.

NI, NII and NIII modes are derived from N-Type Commutations and their typical waveforms are shown in figure 13.

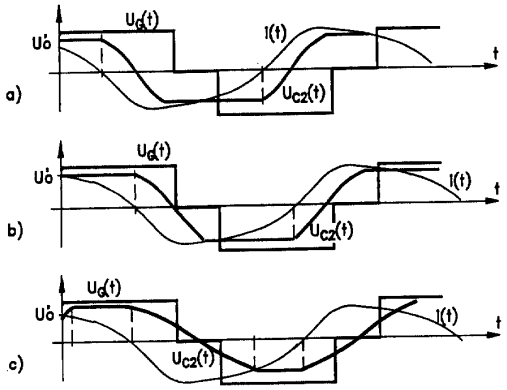

Figure 13. N-Type Commutations a) NI b) NII c) NIII

FI, FII and FIII modes are also derived from F-Type Commutations. Figure 14 shows their typical waveforms.

Finally, MI, MII and MIII modes are derived from M-Type Commutations and their typical waveforms are shown in figure 15 as well.

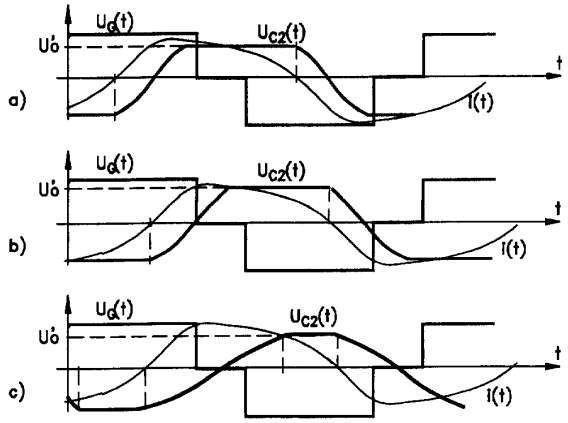

Figure 14. F-Type Commutations a) FI b) FII c) FIII

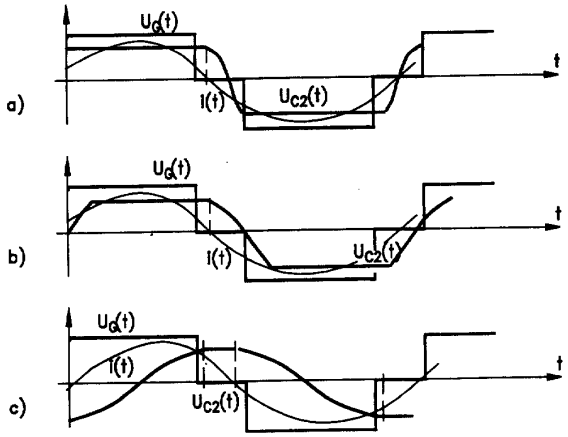

Figure 15. M-Type Commutations a) MI b) MII c) MIII

Each of these modes involves a particular circuits sequence which represents the waveform evolution. From this circuits sequence we can obtain a sequence of mathematical equations. These equations can be solved by numerical methods to obtain the evolutions of the electrical magnitudes in the circuit.

Some of the most important conclusions of the analysis can be seen in figures 16 to 18. Figure 16 connects the normalized output voltage (U_0/U_B) with the normalized switching frequency ($f_{sn}=f_s/f$), the ratio between both resonant capacitors (C_{R1}/C_{R2}) and the duty cycle ($d=\theta/\pi$) being two fixed values. As this figure shows, there are nine different operation zones that correspond to the same number of operation modes, three of them for each conmutation type. The evolution of the N, M and F zones when the ratio C_{R1}/C_{R2} changes can be seen in figure 17. Note that the F-type zone increases when C_{R1}/C_{R2} increases (this zone is the most interesting zone for BJTs, MOS-FETs and IGBTs).

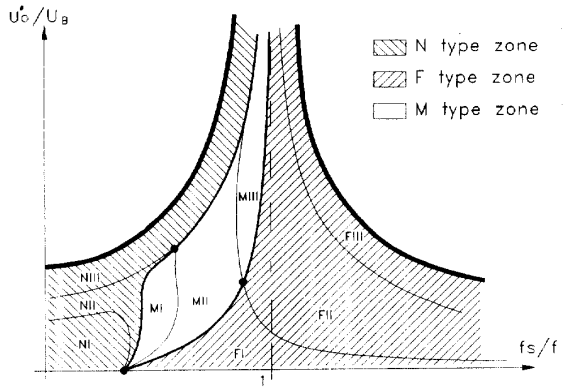

Figure 16. Operating area of the proposed converter and its different zones

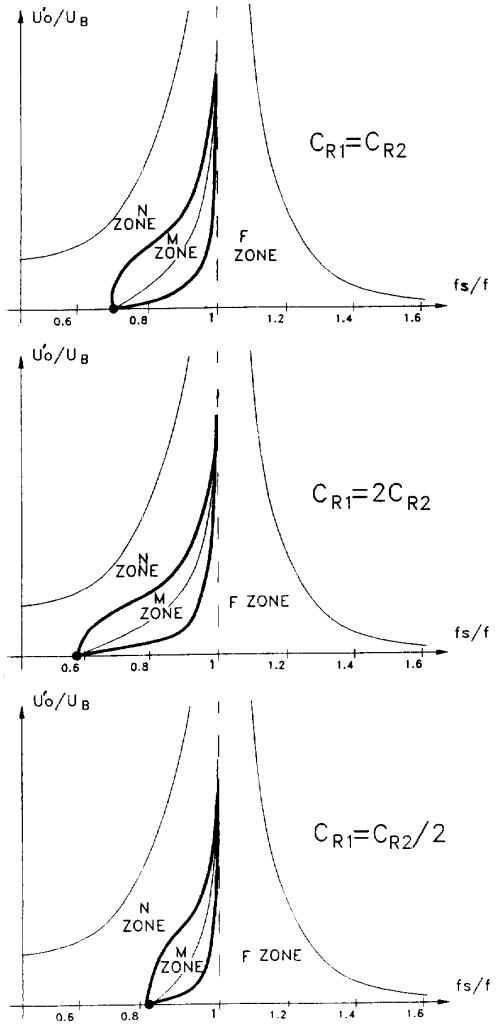

Figure 17. Evolution of the N, M and F zones when the ratio C_{R1}/C_{R2} changes

Figure 18 shows the zones corresponding to two different duty cycles. As this figure shows, the N-type and F-type zones increase when duty cycle increases, and the M-type zone disappears when the duty cycle reaches its maximum value, 0.5.

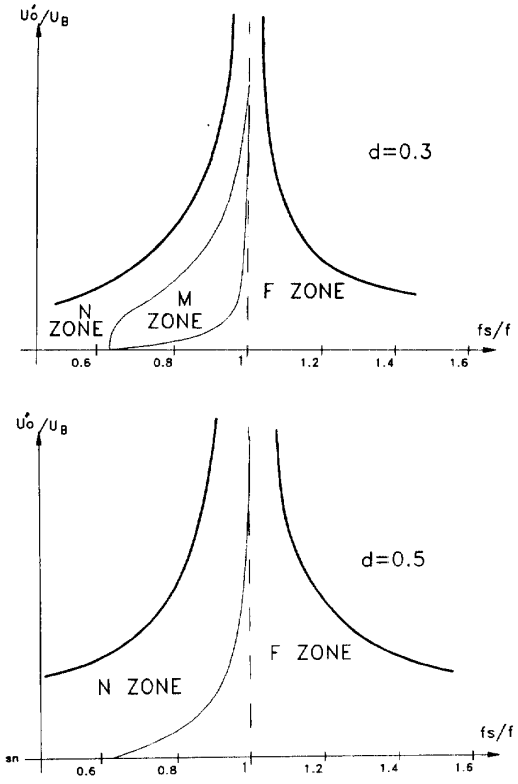

Figure 18. Evolution of the zones when the duty cycle changes a) d = 0.2 b) d = 0.5

DESIGN CRITERIA IN HIGHLY VARIABLE CONDITIONS IN INPUT AND OUTPUT VOLTAGE AND LOAD

The main aim of the design is to maintain high efficiency in very variable conditions in input and output voltage and load. Conduction losses in the power switches and in the resonant elements, and switching losses in the former must thus be minimized.

One of the conclusions to the study carried out is that we have found that no reactive energy is returned from the resonant circuit to the input voltage source when the converter is operating in the M-type conmutation zones. On the other hand, F-type conmutation zones are optimum from the point of view of switching losses, when BJTs, MOSFETs or IGBTs are used as main power switches. Therefore, the boundary between both modes will define the optimum operation conditions. This boundary will be called OPTIMUM SWITCHING LINE.

Figure 19 shows the optimum switching lines for several duty cycles. The normalized output load (R_0/Z) has been included as a second parameter in figure 20, in which both resonant capacitors have been given the same value.

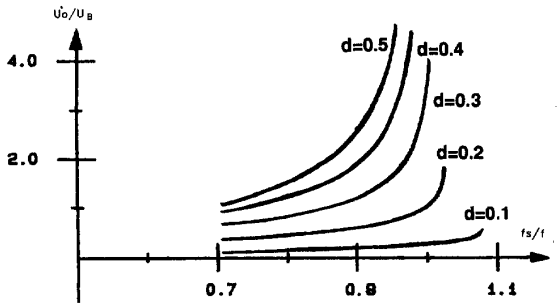

Figure 19. Optimum switching lines for several duty cycles

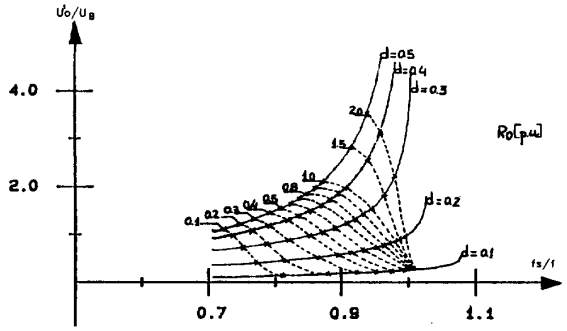

Figure 20. Optimum switching lines with several duty cycles and normalized loads

This graph is the key to design in highly variable conditions in input and output voltage and load. Figure 21 shows the evolution of the operating point in several variable conditions. For example, when the converter changes the normalized output voltage (U_0/U_B) from 3 to 1 the operating point moves from point A to point B (maintaining the load constant). If the normalized load changes from 2 to 0.1, maintaining the normalized output constant, the operating point moves from B to C. The variation in the duty cycle and in the switching frequency can be easily obtained from figure 21 as well.

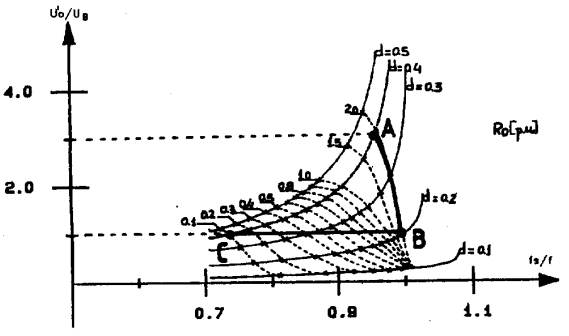

Figure 21. Evolution of the operating point in several variable conditions

DESIGN EXAMPLE

A typical variable output voltage and pulse-load application is shown in figure 22, in which the output voltage changes between 40 and 150 kV and the output current varies between 0 and 1,250 mA. Operation following optimum switching lines leads to figure 23.

In this case, both the duty cycle and the switching frequency change to allow operation always in a optimum switching line. Thus, the duty cycle varies from 0.5 to 0.1 and the switching frequency from 35 to 42.5 kHz. Both resonant capacitors are given equal values in this design.

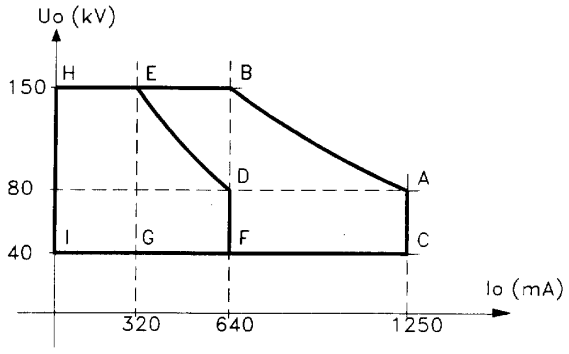

Figure 22. Output voltages and currents in a typical high-voltage pulse-load application

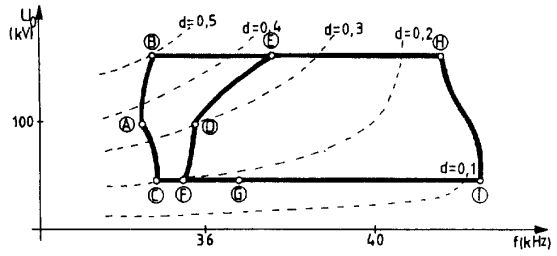

Figure 23. Operating area in the example shown in figure 22 working in the optimum switching line

The main objective of the previous design has been the operation in the optimum switching lines because it implies both low switching and conduction losses. Such an operation leads the converter to be controlled by a mixed PWM and switching frequency control as has been shown in the previous example. However, operation at fixed switching frequency can also be accomplished with low switching losses and with slightly higher conduction losses by designing the converter to operate in F zone but near to the M zone.

EXPERIMENTAL RESULTS

Theoretical study has been verified by simulation, using the "Analog Work Bench" (AWB) from VALID. The circuit and some typical waveforms corresponding to operation near the optimum switching line can be seen in figure 24.

The control circuit to work in the optimun switching lines might seem complicated but in fact is not. A very easy analog circuit has been designed to guarantee operation in optimum switching lines. Figure 25 shows this control circuit.

a)

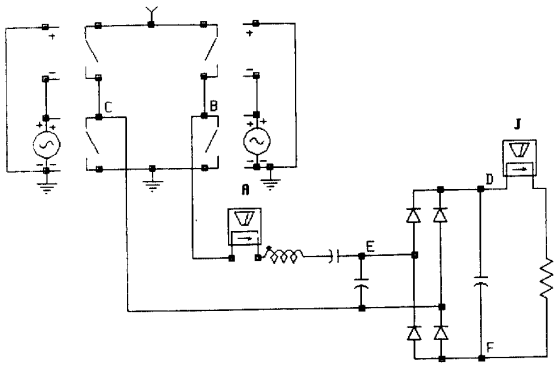

b)

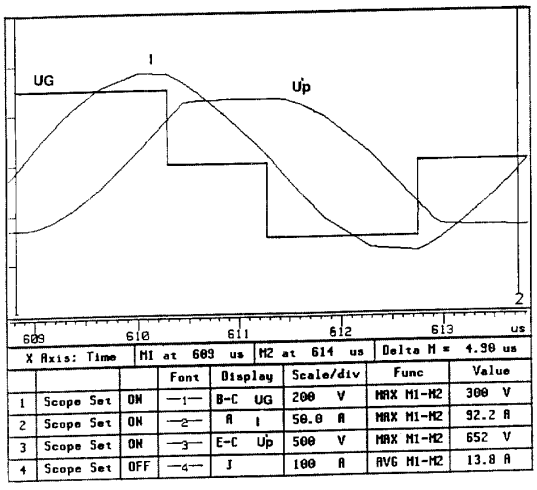

X Axis: Time	M1 at 609 us	M2 at 614 us	Delta M = 4.90 us	
	Font	Display	Scale/div	Func	Value
1 Scope Set ON	—1—	B-C UG	200 V	MAX M1-M2	300 V
2 Scope Set ON	—2—	A I	50.0 A	MAX M1-M2	92.2 A
3 Scope Set ON	—3—	E-C Up	500 V	MAX M1-M2	652 V
4 Scope Set OFF	—4—	J	100 A	AVG M1-M2	13.8 A

Figure 24. Simulated circuit (a) and typical waveform (b)

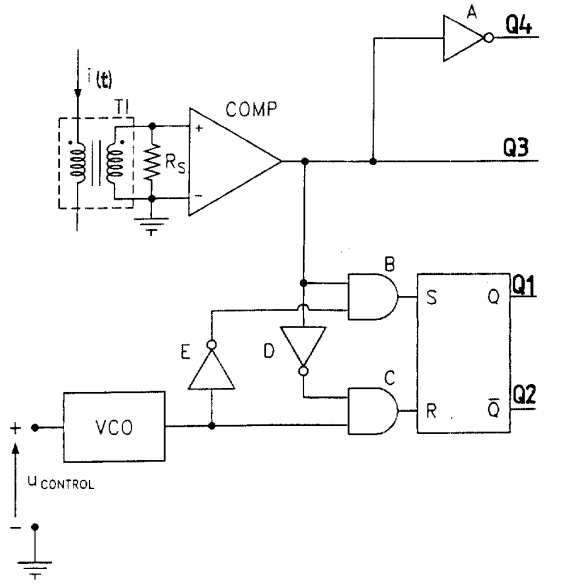

Figure 25. Analog control circuit to operate in optimum switching lines

CONCLUSION

The converter presented in this paper has optimum behaviour for use in high-voltage, pulse-load applications:

- All main parasitics of the high-voltage transformer are integrated into the power topology.

- Diode capacitances are also integrated into the power topology and the power switch capacitances can be integrated into lossless snubbers.

- No reactive energy is returned from the resonant circuit to the input voltage source and, therefore, minimum energy is handled by the resonant circuit and the switches.

- These very desirable conditions can be maintained with very strong variations in the output voltage and current.

The converter operates with Phase-Shifted PWM control at slightly variable frequency with very strong variations in the operating point, but can operate at constant frequency if this behaviour is more desirable than operation in a optimum switching line (with no reactive energy returned to the input source). Nevertheless, in both cases F-type commutations are always guaranteed (lossless snubbers).

REFERENCES

[1] R. Hayner, T.K. Phelps, J.A. Collins and R.D. Middlebrook.
"The Venable Converter: A New Approach to Power Processing".
IEEE-PESC, pp. 92-103, 1976.

[2] A.S. Rostad, C.T. McCown and D.O. Lawrence.
"Application of the Venable Converter to a Series of Satellite TWT Power Processors".
IEEE-PESC, pp. 104-111, 1976.

[3] B.P. Israelsen, J.R. Martin, C.R. Reeve and V.S. Scown.
"A 2.5 kV High-Reliability TWT Power Supply: Design Techniques for High Efficiency and Low Ripple".
IEEE-PESC, pp. 212-222, 1977.

[4] S.D. Johnson, A.F. Witulski and R.W. Erickson.
"Comparison of Resonant Topologies in High-Voltage DC Applications".
IEEE Transactions on Aerospace and Electronic Systems. Vol. 24. nº 3, pp. 263-274, Mayo 1988.

[5] Y. Cheron, H. Foch and J. Salesses.
"Study of a Resonant Converter Using Power Transistors in a 25 kW X-Ray Tube Power Supply".
Proceedings of ESA sessions at IEEE-PESC, pp. 295-306, 1985.

[6] H. Hino, T. Hatakeyama and Nakaoka.
"Digitally Controlled Resonant Converter for X-Ray Generator Utilizing Parasitic Circuit Constants of High Voltage-Transformer". EPE, pp. 361-365, 1989.

[7] H. Hino, T. Hatakeyama and M. Nakaoka.
"Resonant PWM Inverter Linked DC-DC Converter Using Parasitic Impedances of High-Voltage Transformer and Its Applications to X-Ray Generator".
IEEE-PESC, pp. 1212-1219, 1988.

[8] H. Hino, T. Hatakeyama, T. Kawase and M. Nakaoka.
"High-Frequency Parallel Resonant Converter for X-Ray Generator Utilizing Parasitic Circuit Constants of High Voltage-Transformer and Cables".
IEEE INTELEC, pp. 20.5.1 - 20.5.8, 1990.

[9] I. Batarseh, R. Liu, C.Q. Lee and A.K. Upadhyay.
"Theoretical and Experimental Studies of the LCC-Type Parallel Resonant Converter".
IEEE Transactions on Power Electronics, Vol. 5, nº 2. pp. 140-150, January 1988.

[10] S.D. Johnson and R.W. Erickson.
"Steady-State Analysis and Design of the Parallel Resonant Converter".
IEEE Transactions on Power Electronics, Vol. 3. nº 1.pp. 93-104, January 1988.

[11] R.L. Steigerwald.
"A Comparison of Half-Bridge Resonant Converter Topologies".
IEEE Transaction on Power Electronics, Vol. 3, nº 2.pp. 174-182, April 1988.

[12] F. Tsai, J. Sabate and F.C. Lee.
"Constant-Frequency, Zero-Voltage-Switched, Clamped-Mode Parallel-Resonant Converters".
IEEE INTELEC, pp. 16.4.1 - 16.4.7, 1990.

[13] R.L. Steigerwald.
"High-Frequency Resonant Transistor DC-DC Converters".
IEEE Transactions on Industrial Electronics, Vol. IE-31, nº 2, pp.181-191, May 1984.